Lymphocytes eject interferogenic mitochondrial DNA webs in response to CpG and non-CpG oligodeoxynucleotides of class C

Björn Ingelsson[a], Daniel Söderberg[b], Tobias Strid[a], Anita Söderberg[a,1], Ann-Charlotte Bergh[a], Vesa Loitto[a], Kourosh Lotfi[b,c], Mårten Segelmark[b,d], Giannis Spyrou[a], and Anders Rosén[a,2]

[a]Department of Clinical and Experimental Medicine, Linköping University, SE-581 85 Linköping, Sweden; [b]Department of Medical and Health Sciences, Linköping University, SE-581 85 Linköping, Sweden; [c]Department of Hematology, Linköping University, SE-581 85 Linköping, Sweden; and [d]Department of Nephrology, Linköping University, SE-581 85 Linköping, Sweden

Edited by Dennis A. Carson, University of California, San Diego, La Jolla, CA, and approved December 11, 2017 (received for review July 11, 2017)

Circulating mitochondrial DNA (mtDNA) is receiving increasing attention as a danger-associated molecular pattern in conditions such as autoimmunity, cancer, and trauma. We report here that human lymphocytes [B cells, T cells, natural killer (NK) cells], monocytes, and neutrophils derived from healthy blood donors, as well as B cells from chronic lymphocytic leukemia patients, rapidly eject mtDNA as web filament structures upon recognition of CpG and non-CpG oligodeoxynucleotides of class C. The release was quenched by $ZnCl_2$, independent of cell death (apoptosis, necrosis, necroptosis, autophagy), and continued in the presence of TLR9 signaling inhibitors. B-cell mtDNA webs were distinct from neutrophil extracellular traps concerning structure, reactive oxygen species (ROS) dependence, and were devoid of antibacterial proteins. mtDNA webs acted as rapid (within minutes) messengers, priming antiviral type I IFN production. In summary, our findings point at a previously unrecognized role for lymphocytes in antimicrobial defense, utilizing mtDNA webs as signals in synergy with cytokines and natural antibodies, and cast light on the interplay between mitochondria and the immune system.

mitochondrial DNA release | immune DNA sensing | lymphocyte signaling | DAMP | CpG-C

Cellular receptors in our innate immune system such as natural antibodies on B cells, scavenger receptors, and recently discovered immune DNA sensors are programmed to recognize, and respond to, pathogen-associated molecular patterns (PAMPs) present on foreign microbes, as well as recognition of danger-associated molecular patterns (DAMPs), released by damaged cells (1, 2). Recently, it was shown that mitochondria, having an ancestral bacterial origin, release DAMP structures including mitochondrial DNA (mtDNA), ATP, mitochondrial transcription factor A (TFAM), *N*-formyl peptides, succinate, and cardiolipin (3). Released mtDNA participates in inflammatory responses via different pathways. In the cGAS/STING pathway, mtDNA participates in cell-intrinsic triggering of innate immune responses and antiviral signaling, and triggers type I IFN release (4–6). Similar to bacterial and viral DNA, mtDNA is enriched in unmethylated CpG dinucleotide motifs, which exhibit strong immunostimulatory effects (7). Unmethylated CpG oligodeoxyribonucleotides (ODNs) are recognized by endosomal Toll-like receptor 9 (TLR9), which is expressed at high levels in plasmacytoid dendritic cells and B cells. TLR9-ligand binding stimulates proliferation, Ig production, and secretion of IL-6, IL-12, and IFN-γ (8–11). mtDNA also stimulates proinflammatory cytokine release via activation of the AIM2 and NLRP3 inflammasomes (12, 13).

The spectacular neutrophil discharge of decondensed genomic DNA strands complexed with antibacterial proteins, such as neutrophil elastase and myeloperoxidase, termed neutrophil extracellular traps (NETs), was previously found to be triggered by bacterial PAMPs and phorbol myristate acetate (PMA) (14). Release was associated with a particular form of cell death, NETosis, without spreading of harmful granule enzymes and histones (14, 15). Later, it was observed that extracellular traps (ETs) could be generated by live cells that released mtDNA instead of nuclear DNA (16–19). Notably, Itagaki et al. (20) found that cell-free mtDNA, released in trauma patients, itself induced classical, suicidal, NETosis via a reactive oxygen species (ROS)-dependent TLR9 pathway. Although beneficial for pathogen clearance, circulating DNA constitutes a potential risk for autoantibody induction if not rapidly cleared. Both nuclear and mtDNA ETs show proinflammatory characteristics and have been detected in clinical conditions such as autoimmunity, HIV, and cancer (21–24).

In this study, we report the previously unrecognized finding that lymphocytes [B cells, T cells, natural killer (NK) cells], as well as monocytes and neutrophils, upon treatment with CpG-C and non–CpG-C, rapidly release mtDNA as long elastic filaments that we call webs. The web release was induced in a pathway independent from B-cell antigen receptor (BCR), TLR9, STING, and AIM2 signaling, independent from ROS and cell death (apoptosis, necrosis, necroptosis, autophagy). Isolated web protein composition analyzed by mass spectrometry was different from NETs. Once released, the mtDNA webs primed

Significance

Release of pathogen- and danger-associated molecular patterns (PAMPs and DAMPs) contributes to inflammatory responses and antiviral signaling. Mitochondrial DNA (mtDNA) is a potent DAMP molecule observed in blood circulation of trauma, autoimmune, HIV, and certain cancer patients. Here, we report a previously unrecognized lymphocyte feature that CpG and non-CpG oligodeoxynucleotides of class C promptly induce release of mtDNA as extracellular web-like structures. Lymphocyte mtDNA webs provoked antiviral type I IFN production in peripheral blood mononuclear cells but were devoid of bactericidal proteins. Notably, cells remained viable after the release. Our findings imply an alternative role for lymphocytes in antiviral signaling by utilizing their mtDNA as a rapid signaling molecule to communicate danger.

Author contributions: B.I., D.S., G.S., and A.R. designed research; B.I., D.S., T.S., A.S., A.-C.B., V.L., and A.R. performed research; K.L. and G.S. contributed new reagents/analytic tools; B.I., D.S., T.S., A.S., A.-C.B., V.L., K.L., M.S., G.S., and A.R. analyzed data; and B.I., G.S., and A.R. wrote the paper.

The authors declare no conflict of interest.

This article is a PNAS Direct Submission.

[1]Deceased March 5, 2017.

[2]To whom correspondence should be addressed. Email: anders.rosen@liu.se.

This article contains supporting information online at www.pnas.org/lookup/suppl/doi:10.1073/pnas.1711950115/-/DCSupplemental.

www.pnas.org/cgi/doi/10.1073/pnas.1711950115

antiviral type I IFN secretion in peripheral blood mononuclear cells (PBMCs). Thus, a scenario emerges where immune cells may utilize mtDNA as rapid danger messenger molecule acting in synergy with cytokines and natural antibodies.

Results

B Lymphocytes Release Extracellular DNA Webs After Sensing GC-Rich Oligonucleotides. Natural antibodies recognizing modified epitopes on proteins, lipids, and DNA are produced by innate B1-like B cells and by chronic lymphocytic leukemia (CLL) B cells (25, 26). DNA released into circulation is a potentially harmful DAMP, and its removal is essential to avoid autoimmune reactions (24). In the process of studying binding of natural autoantibodies derived from CLL B cells (26, 27) to NET structures, we observed that these CLL B cells not only produced antibodies to NETs, but also could release ET-like structures themselves.

This finding prompted us to search for potential inducers of B-cell ETs. Unexpectedly, in a panel of 18 known NET inducers and B-cell activators (Fig. 1 and *SI Materials and Methods*), CpG oligonucleotide of class C (ODN 2395; hereinafter referred to as CpG-C, unless otherwise stated) was the only stimuli that induced release of ET-like structures (Fig. 1 *A*–*C*). These webs were sensitive to DNase treatment, implicating DNA content (Fig. 1*D*). Untreated cells or CpG-C treatment of isolated cell supernatants, in which cells were removed by centrifugation, did not generate these fibrous DNA structures (Fig. 1 *E* and *F* and Fig. S1*A*). These B-cell DNA webs were flexible and fragile, that is, sensitive to paraformaldehyde fixation, compared with PMA-induced NETs. Therefore, onward analyses of B-cell DNA webs were performed by live-cell fluorescence microscopy and agarose gel electrophoresis. Released DNA isolated from cell culture media revealed a distinct large-sized DNA fragment exclusively found in CpG-C–exposed cultures as analyzed in agarose gel electrophoresis (Fig. 1*G*).

We expanded the analysis to a panel of $CD5^+/CD19^+$ leukemic B-cell samples isolated from 14 treatment-naive CLL patients, as well as to six $CD19^+/CD20^+$ and two B1-like $CD5^+/CD19^+$ B-cell samples from healthy blood donors and found all to produce DNA webs in response to CpG-C. Thus, DNA release was not restricted to leukemic B cells or B1-like B cells. In expanded analyses to other PBMC subpopulations, we found that all tested cells (B cells, T cells, NK cells, and monocytes) released DNA webs in response to CpG-C (Fig. 1*H* and Fig. S1*B*). In addition, neutrophils also released CpG-C–induced DNA webs that appeared different from PMA-induced NETs (Fig. 1 *I* and *J*). Notably, the electrophoretic migration pattern of CpG-C–induced DNA webs in agarose gels was compared with PMA-induced NETs and found to be markedly different. DNA released upon CpG-C treatment migrated as a uniform-sized fragment, while PMA-induced NETs consisted of large-sized DNA with strongly retarded gel entry, implicating a different and larger structural composition (Fig. 1*K*, lanes 2 and 3). Inhibition of NADPH oxidase by apocynin did not prevent CpG-C–stimulated neutrophils from releasing DNA webs, whereas PMA-induced NETs were abolished, indicating a different release mechanism (Fig. 1*K*, lanes 5 and 6, and Fig. S1*C*). We also tested whether nonimmune cells could generate webs. However, CpG-C did not trigger web release from primary foreskin fibroblasts, HepG2 liver carcinoma epithelial cells, and HEK 293 embryonic kidney epithelial cells (Fig. S1*D*). Therefore, we decided to study the DNA release from B cells in detail.

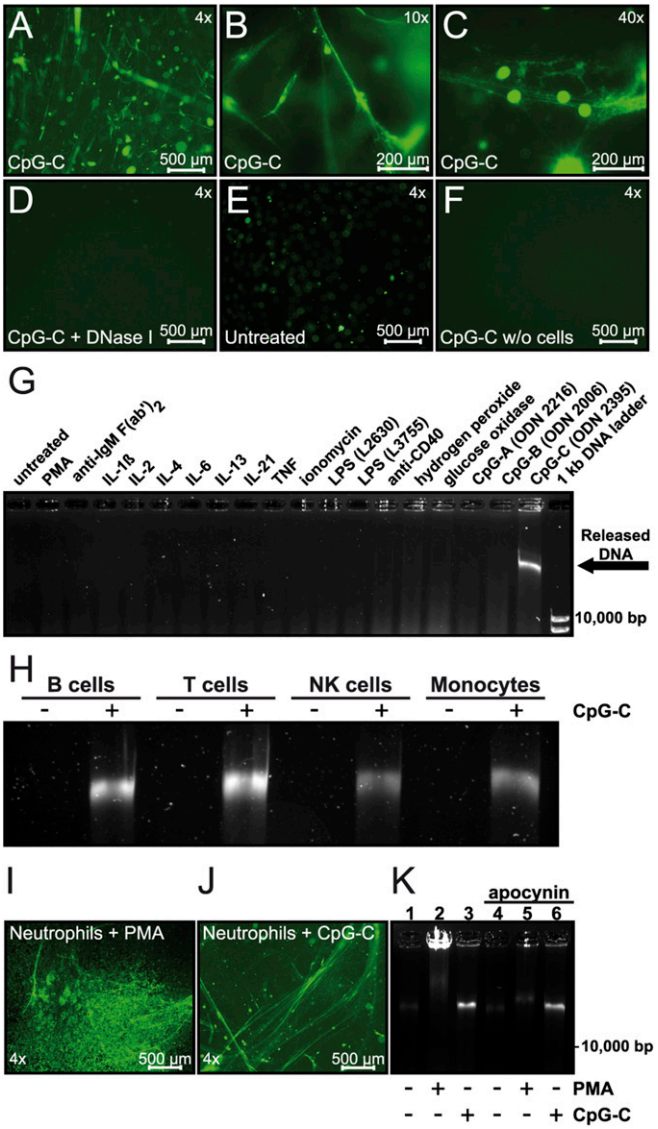

Fig. 1. CpG-C ODN prompts B cells to release DNA as long extracellular webs. (*A*–*C*) Visualization of extracellular DNA in cell culture medium after treatment of CLL B cells with CpG-C using live-cell microscopy with Nikon Eclipse with a 4× objective, and Zeiss Axiovert with 10× and 40× objectives, respectively. (*D*) Treatment of released DNA with DNase I for 30 min. (*E*) Extracellular nucleic acid staining in untreated control samples. (*F*) CpG-C ODN in cell supernatants after removal of cells. Cells were incubated in cell culture media for 3 h before cells were removed by centrifugation and further incubated with CpG-C for 3 h. (*G*) Agarose gel electrophoresis separation of collected extracellular DNA from cell supernatants after incubation of CLL B cells with indicated stimuli revealed a characteristic DNA fragment present only in samples from CpG-C–treated cells (indicated by an arrow). (*H*) Analysis of DNA webs produced by B cells, T cells, NK cells, and monocytes in agarose gels. (*I* and *J*) Microscope images (4× objective) showing DNA release from PMA- and CpG-C–stimulated neutrophils, respectively. (*K*) Agarose gel electrophoresis of extracellular DNA collected from neutrophils treated with PMA or CpG-C in the presence or not of apocynin.

Released B-Cell Webs Are of mtDNA Origin. DNA sequencing of the characteristic fragment observed in Fig. 1*G* disclosed high abundance of mtDNA, a finding that was verified by PCR using primers specific for mitochondrial or nuclear DNA (Fig. 2*A* and Fig. S2 *A* and *B*). The apparent size of the released mtDNA was, however, significantly larger than expected for mtDNA. Purification of released DNA by removal of cell culture media components, changed the apparent size to that of purified mtDNA (Fig. 2*B*). A reverse-step experiment was performed in which purified mtDNA was added to cell culture media. This resulted in a retarded migration and an apparent size similar to that of uncleaned webs (Fig. 2*B*), suggesting that presence of cell culture media affects mtDNA mobility. We also observed that DNA

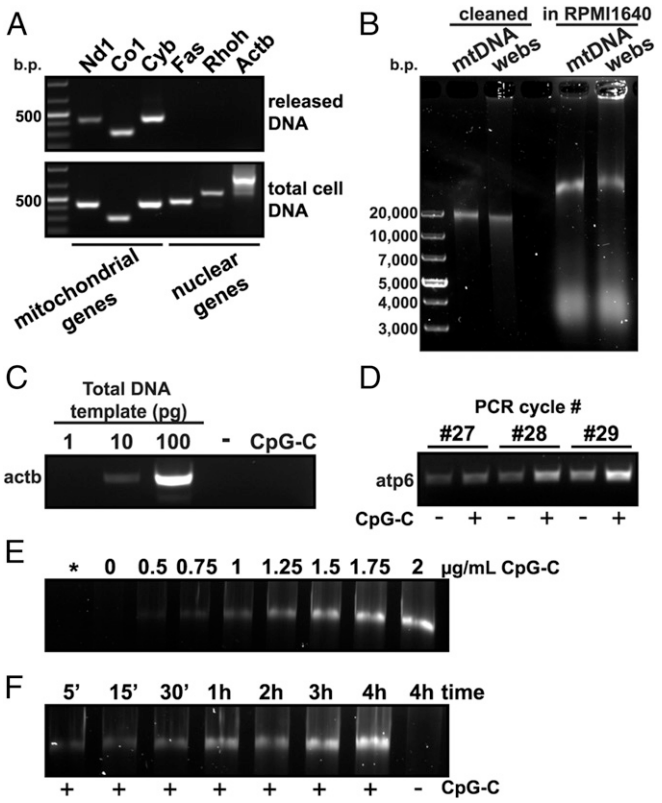

Fig. 2. Rapid dose-dependent release of mtDNA from B cells upon CpG-C exposure. (*A*) PCR analysis of the characteristic band observed in Fig. 1*G* with specific primers for both mitochondrial and nuclear-encoded genes using total cell DNA as control. (*B*) Comparison of purified mtDNA and isolated mtDNA webs in agarose gels. DNA was either purified by removal of cell culture media components ("cleaned") or mixed with RPMI 1640 before electrophoresis. (*C*) PCR analysis of total isolated DNA released from untreated and CpG-C–treated cells using a primer specific for a nuclear encoded gene (actb). Total DNA isolated from CLL B cells at different template amounts was used as positive control. (*D*) PCR analysis of DNA released from untreated and CpG-C–treated cells using a primer specific for a mitochondria encoded gene (atp6). The analysis was made by varying the number of PCR cycles, and the ratio CpG-C treated/untreated was calculated by measuring band intensities ($n = 4$). (*E*) Agarose gel separation of extracellular DNA collected from cells treated with increasing amounts of CpG-C revealed concentration dependence of mtDNA release. The asterisk (*) denotes the medium control containing CpG-C in the absence of cells. (*F*) A representative gel showing the time dependence of mtDNA release from B cells upon CpG-C treatment during 4 h ($n = 3$).

migration was hampered by presence of SYTOX Green nucleic acid stain (Fig. S2*C*). Of note, PCR analysis of DNA isolated from collected supernatant, using nuclear DNA-specific primers, did not show presence of any nuclear DNA (Fig. 2*C*). In contrast, mtDNA could be amplified in <1% of the sample (Fig. 2*D*). Spontaneous release of mtDNA fragments has been previously reported (28), and we also observed that mtDNA was amplified in untreated samples, albeit to a significantly lower extent (mean ratio of CpG-C treated/untreated, 2.0; SD, ±0.4; $P < 0.005$; $n = 4$). However, since no large-size DNA was observed in supernatants of untreated cells (Fig. 1*G*), our results show that CpG-C specifically induce release of webs consisting of full-size mtDNA rather than fragments. Copy number analysis of DNA remaining in cells after CpG-C treatment, using droplet digital PCR, did however not reveal any significant change in mtDNA copy number compared with untreated cells (Fig. S2*D*).

Increasing concentrations of CpG-C resulted in dose-dependent release of mtDNA from B cells (Fig. 2*E* and Fig. S2*E*), and kinetic analysis revealed increase of mtDNA webs within cell supernatants over time (Fig. 2*F*). Of note, CpG-C was localized rapidly in the cells (Fig. S2*F*) but appeared not to align with the released mtDNA as analyzed with FITC-labeled CpG-C (Fig. S2*G*).

mtDNA Web Casting in B Cells Is Uncoupled from Cytokine Release. CpG-ODNs are known ligands of TLR9, but interestingly CpG recognition by TLR9 differs between immune cells depending on the ODN class (29). These classes differ both in the primary and secondary structure (Fig. 3*A*). B cells are known to release cytokines in response to ODNs of B and C classes (8). As we only found CpG of the C class to induce mtDNA-web ejection from B cells, we wanted to analyze the involvement of TLR9 in this event further. Secretion of different cytokines, IL-10, IL-1, IL-6, IFN-α2, and TNF (Fig. 3*B* and Fig. S3 *A–D*), after stimulation of CLL B cells with CpG-A, CpG-B, and CpG-C for 6 h, was compared with mtDNA web release data described in Fig. 1*G*. CpG-A neither generated IL-10 nor webs, whereas both CpG-B and CpG-C provoked IL-10 secretion, but remarkably only CpG-C induced mtDNA webs. Negative controls of TLR9 pathway signaling, ODNs lacking the CpG structural motif (non-CpG; e.g., GpC-B and GpC-C), did not induce IL-10 secretion compared with untreated cells (Fig. 3*B*), indicating the importance of the CpG-structural motif for cytokine production via TLR9. Chloroquine, an inhibitor of TLR9 signaling, abolished IL-10 secretion from CpG-B– and CpG-C–stimulated cells, verifying TLR9 pathway block (Fig. 3*B*). Importantly, chloroquine did not compromise CpG-C–induced mtDNA release (Fig. 3*C*), suggesting an endosomal TLR9-independent pathway.

mtDNA Webs Are Induced in a TLR9-Independent Pathway. The observation that CpG-B induced TLR9-dependent cytokine secretion, but not mtDNA web release, prompted us to carefully analyze different CpG ODN classes for the ability to induce mtDNA webs. The amount of released webs from CLL B cells treated with 1.25 µg/mL (180 nM) CpG-C for 2 h was used as a reference. CLL B cells were also treated at 180 or 360 nM with CpG-A, CpG-B, GpC-C, and the inhibitory ODN TTAGGG (A151) known to block CpG signaling. Remarkably, the non–CpG-C control, GpC-C, induced mtDNA release in a dose-dependent manner (Fig. 3*D* and Fig. S3*D*), emphasizing that the CpG-motif per se is not crucial for mtDNA web release. No web release was observed for CpG-A, CpG-B, and A151, as shown by gel electrophoresis and immunofluorescence (Fig. 3*D* and Fig. S3*E*). Since only C-class ODNs were found to stimulate webs, two additional C-class ODNs (ODN D-SL03 and ODN M362) as well as a P-class ODN (ODN 21798) were analyzed. P-class ODN 21798 is similar to the CpG-C ODN 2395 used in our previous experiments, but holds an extra CpG motif and one additional stem-loop motif (Fig. S3*F*). Both ODN D-SL03 and ODN 21798 induced web release, while no or very low amounts of webs could be observed after stimulation by ODN M362 (Fig. S3 *G–I*). The ODN sequences and secondary structures (Fig. 3*A* and Fig. S3*F*) indicate a common GC-rich stem-loop motif at the 3′ end for the stimulating ODNs, reminiscent of certain viral G-rich Y-form DNA motifs (30).

Combination of ODNs of the other classes with CpG-C did not reduce web release compared with stimulation by CpG-C alone (Fig. S3*J*), indicating that CpG-C targets a unique sensor to which no competitive binding of CpG-A, CpG-B, nor A151 occur. A TLR9-independent pathway is further supported by the finding that additional inhibitors of TLR9 signaling, rolipram and wortmannin (31, 32), also did not prevent the release of mtDNA upon CpG-C treatment (Table 1 and Fig. S4*A*). In addition to endosomal expression, B cells express TLR9 on the plasma membrane (33). However, we observed no inhibitory (or stimulatory) effect of B-cell DNA web formation in the

presence of anti-TLR9 antibodies (Fig. S4*A*), despite the fact that both CpG-C and the TLR9 antibody did bind to cell surface (Fig. S4*B*). We found that B cells and T cells produced mtDNA webs at similar levels (Fig. 1*H*). However, TLR9 is known to be expressed at higher levels in B cells (10) and immunoblotting using a TLR9-specific antibody revealed much less TLR9 in T cells and neutrophils compared with B cells (Fig. 3*E*), also suggesting a TLR9-independent mechanism of web release.

B-Cell Webs Induce Release of Type I IFN from PBMCs. As mtDNA has been reported to act as a DAMP molecule with interferogenic and proinflammatory properties, we wanted to examine whether B-cell mtDNA webs also could elicit a similar response. Webs from GpC-C–treated CLL B cells were collected and incubated with PBMCs (*Materials and Methods*). PBMCs exposed to webs for 16 h released significant amounts of type I IFN (IFN-α) ($P < 0.005$; Fig. 4*A*) but not IL-1β (Fig. S5 *A* and *B*). Importantly, B-cell supernatants devoid of webs (i.e., supernatants from CLL cells not exposed to GpC-C; "untreated") could not induce IFN-α secretion (Fig. 4*A*). Interestingly, DNase treatment of webs amplified the IFN-α production ($P < 0.0005$). Although the characteristic web fragment in agarose gels could not be observed after DNase treatment, the gene for mitochondrial cytochrome *b* could still be amplified by PCR (Fig. S5 *C–E*). DNase digest DNA into oligonucleotides and mononucleotides, and obviously these smaller web fragments were more interferogenic. The GpC-C control induced detectable IFN-α secretion but to a significantly lower extent than webs (webs vs. GpC-C control, $P < 0.05$), most likely due to GpC-C retention in the sample. GpC-C is not known to induce IFN-α by itself, but as GpC-C stimulate PBMCs to release webs, GpC-C contamination within the web sample could contribute to the observed IFN-α (Fig. 4*A*). The supernatant of GpC-C–exposed CLL B cells used for PBMC stimulation contained no IFN-α (Fig. 4*B*).

mtDNA Web Casting Is Inhibited by Zn^{2+} and Hypothermia. Potential mechanisms behind B-cell mtDNA web release were investigated by intervening cellular pathways with appropriate inhibitors (Table 1). For comparison, we analyzed their capacity of inhibiting PMA-induced NETs in parallel (Fig. S6*A*). The results are presented in Fig. 3*F* and Figs. S4 and S6*B*. Strikingly, although several inhibitors effectively inhibited NET release, only treatment with $ZnCl_2$ prevented CpG-C–induced B-cell webs (Fig. 3*F*). Importantly, cell viability was not compromised by $ZnCl_2$ (Fig. S4 *D* and *E*). Hypothermia (+4 °C) showed similar inhibition of web formation (Fig. 3*F*).

The mode of action of inhibitors along with affected pathways is illustrated in Fig. 5. To summarize, we found no effect on web release by blocking BCR, TLR9, cGAS/STING, and AIM2 inflammasome signaling pathways. Inhibitors of cell death (apoptosis, necrosis, necroptosis, autophagy), ROS formation, and endocytosis were also ineffective. Cyclosporin A, previously reported to inhibit release of mtDNA fragments (28), did not affect web release.

Although hypothermia and zinc sensitivity specify active biological processes, both treatments intervene with multiple cellular processes and insight in mechanistic details of mtDNA web casting renders further studies.

mtDNA Web Casting Is Not Accompanied by ROS/Reactive Nitrogen Species nor Cell Death. Inhibitors and scavengers of ROS had no effect on mtDNA release (Table 1), which argues for a ROS-independent mechanism. To verify this, various reactive species, that is, hydrogen peroxide, peroxynitrite, hydroxyl radicals, nitric

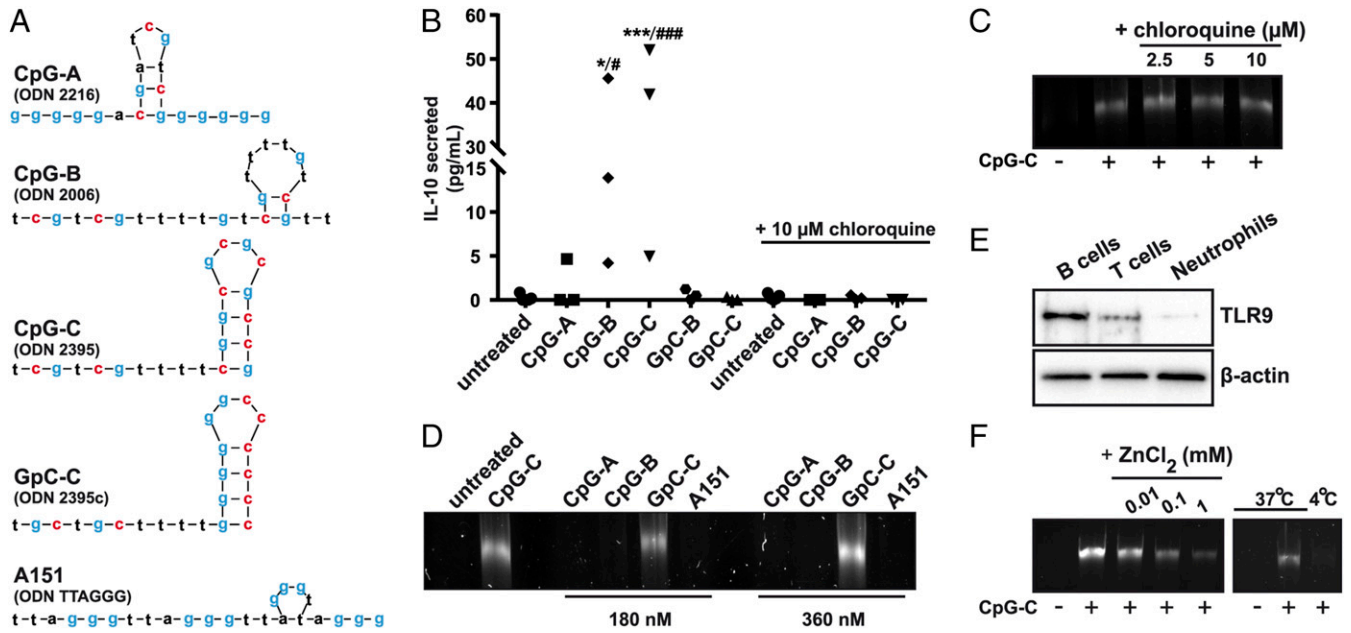

Fig. 3. Impact of different CpG classes on cytokine secretion and web release. (*A*) Sequences and mfold predictions of secondary structures of the ODNs used. The structures with the lowest Gibbs free energy for each ODN are presented. Cytosine and guanine bases are highlighted. (*B*) IL-10 concentrations in the supernatants of CLL B cells after 6 h of incubation with indicated ODNs with or without the presence of chloroquine (10 μM). Data are expressed as picograms per milliliter and show the mean plotted for each individual experiment ($n = 3$). $^{*}P < 0.05$, $^{***}P < 0.0005$ (one-way ANOVA followed by Dunnett's post hoc test), $^{\#}P < 0.05$, $^{\#\#\#}P < 0.0005$ [one-way ANOVA followed by Sidak's post hoc test for pairwise comparisons (CpG-B vs. CpG-B plus chloroquine; CpG-C vs. CpG-C plus chloroquine)]. (*C*) The effect of chloroquine on mtDNA web release after incubation with 1.25 μg/mL CpG-C was analyzed by agarose gel electrophoresis and DNA staining ($n = 3$). (*D*) Extracellular DNA collected from cell supernatants after 2-h incubation of B cells with indicated ODNs at two different concentrations was analyzed using agarose gel electrophoresis and DNA staining. CpG-C (180 nM corresponding to 1.25 μg/mL) was used as a reference ($n = 3$). (*E*) Immunoblot showing the presence of TLR9 in B cells, T cells, and neutrophils. Proteins corresponding to equal number of cells were separated using SDS/PAGE and immunoblotting toward actin was used as a loading control. (*F*) The effect of $ZnCl_2$ and hypothermia on mtDNA web release analyzed using agarose gel electrophoresis.

Table 1. Effects of signal pathway inhibitors on B-cell mtDNA web release and NET formation

Treatment	Mode of action	Concentrations tested	Inhibition of mtDNA web release	Inhibition of NETs
TLR9 signaling inhibitors				
Chloroquine	Prevents endosome formation and TLR9 signaling	10 μM	No	No
Rolipram	PDE4 inhibitor; inhibits intracellular TLR9 signaling	20 μM	No	No
Wortmannin	PI3K and autophagy inhibitor; also inhibits the uptake and colocalization of CpG DNA with TLR9	4–10 μM	No	No
Anti-TLR9 antibody	Binds to TLR9 on plasma membrane	10 μg/mL	No	NT
BCR signaling inhibitors				
PP2	Inhibits Src family kinases	1 μM	No	No
Syk inhibitor II	Inhibitor of Syk; can also inhibit PKCε, PKCβII, ZAP-70, Btk, and Itk at higher concentrations	10 μM	No	Yes**
ROS inhibitors/scavengers				
Apocynin	Inhibitor of NADPH oxidase activity	0.1–1 mM	No	Yes**
DPI	Inhibitor of NADPH oxidase activity	2.5–10 μM	No	Yes**
Catalase	Catalyzes the decomposition of hydrogen peroxide to water and oxygen	1,000 U/mL	No	Yes**
PEG-catalase	PEG-catalase can cross plasma membrane and act intracellular	1,000 U/mL	No	Yes*
Superoxide dismutase (SOD)	Catalyzes the dismutation of superoxide radicals to hydrogen peroxide and molecular oxygen	50–200 U/mL	No	No
PEG-SOD	PEG-SOD can cross the plasma membrane and act intracellular	200 U/mL	No	No
N-Acetyl cysteine (NAC)	Antioxidant	5 mM	No	No
Deferoxamine mesylate	Dextran conjugated; iron chelator; inhibitor of Fenton chemistry	1,000 μM	No	No
Ferrostatin-1	Inhibitor of ferroptosis acting as a lipid ROS scavenger	5 μM	No	No
Rotenone	Modulator of mitochondrial electron transport chain	2.5 μM	No	No
MitoQ	Mitochondria-targeted antioxidant	1 μM	No	No
Inhibitors of cell death and endocytosis				
Nec1	Inhibitor of necroptosis	10 μM	No	No
Q-VD-OPh	Pan-caspase inhibitor	10 μM	No	No
Cytochalasin D	Depolymerizes F-actin; inhibitor of endocytosis	2.5–10 μM	No	Yes**
Dansylcadaverine	Inhibitor of clathrin-dependent endocytosis	25–100 μM	No	No
Miscellaneous				
Cyclosporin A	Immunosuppressant; also found to inhibit the release of mtDNA fragments by inhibiting of mitochondria pore opening	1–40 μM	No	NT
Hypothermia	Affects multiple cellular processes, that is, inhibition of endocytosis	Incubation at +4 °C	Yes	Yes**
Quinacrine	Inhibitor of inflammation; nonspecific inhibitor of cGAS/STING signaling	5–10 μM	No	NT
$ZnCl_2$	Inhibits several cellular processes including cysteine proteases, iron uptake, lymphocyte proliferation, MAP kinases, endonucleases, and TNF-induced cytolysis	0.01–1 mM	Yes	Yes*

*$P < 0.05$; **$P < 0.01$; NT, not tested.

oxide, and peroxy radicals, were probed. Indeed, neither CLL B cells nor neutrophils were found to increase ROS/reactive nitrogen species (RNS) after CpG-C stimulation (Fig. 6*A*). However, as expected, high ROS levels were observed in PMA-stimulated neutrophils, used as a positive control. Generation of mitochondrial superoxide was analyzed using MitoSOX Red, which specifically targets mitochondria. No production of mitochondrial superoxide was observed in CpG-C–stimulated cells, while PMA induced an intense formation of superoxide in neutrophils (Fig. S6 *C* and *D*).

mtDNA web release could not be blocked by inhibitors of cell death (Q-VD-OPh, necrostatin-1, and wortmannin; Table 1 and Fig. S4*A*), and analysis of necrosis revealed no effect after CpG-C exposure. This is in clear contrast to PMA treatment of neutrophils, which had a potent cytotoxic effect (Fig. 6*B*). Monitoring cell viability and apoptosis within the same sample did not reveal any effect on cell viability upon CpG-C treatment (Fig. 6*C*). No significant variations in caspase 3/7 activity were observed, in contrast to staurosporine-exposed cells that had a high caspase 3/7 activity.

In addition, active metabolism was not affected by CpG-C compared with untreated cells, while metabolism in staurosporine-exposed cells was hampered (Fig. S6*E*). Similarly, cellular ATP levels were not compromised compared with untreated and CpG-B–treated cells, suggesting no mitochondrial dysfunction (Fig. 6*D*). Inhibition of the mitochondrial electron transport

chain by antimycin A or rotenone did, however, completely abolish ATP production.

B-Cell Webs Are Devoid of Bactericidal Proteins. Considering that the fragile nature of released mtDNA may preclude isolation of mtDNA web-associated proteins using methods previously described for NET protein isolation (34), we developed an extracellular DNA isolation method taking advantage of the interaction between DNA and silicate glass beads (*SI Materials and Methods*). This method allowed identification of the majority of the PMA-induced NET-associated proteins previously described (34), including several bactericidal proteins (Table S1), thus verifying the reliability of our method. We analyzed isolated webs from 10 CpG-C–treated CLL B-cell cultures and 10 control samples [e.g., untreated ($n = 7$) and CpG-A treated ($n = 3$)]. However, none of the proteins associated with NETs could be found within B-cell mtDNA webs (Dataset S1). The proteins presented in Dataset S1 represent those proteins that were found to differ in spectral counts by a factor of >1.5. It should be noted that the samples overall contained very small amounts of proteins, and some of the identified proteins should possibly be regarded as contaminants (e.g., keratin and complement C4). However, the webs are clearly devoid of proteins with antimicrobial properties. The absence of antibacterial proteins in the webs underline the difference to NETs. The antibacterial properties of NETs and mtDNA webs were also tested on *Escherichia coli*. Released B-cell webs were incubated with *E. coli* DH5α and found not to compromise the number of colony-forming bacteria (Fig. 6*E*). Thus, we conclude that B-cell mtDNA webs are unique and differ from previously reported NETs of nuclear DNA or mtDNA origin.

The mitochondrial transcription factor TFAM regulates the degree of mtDNA packing into nucleoids (35). As mass spectrometry did not reveal any TFAM associated with the webs, we made a more dedicated analysis of TFAM using immunoblotting. We could not detect any TFAM in the extracellular fraction (cell supernatant-containing webs) measured after 4 h of CpG-C treatment, indicating low, if any, amounts of TFAM to be released along with the webs (Fig. 6*F*). However, we observed an intense increase of intracellular TFAM levels in CpG-C–exposed cells compared with untreated cells (Fig. 6*F*). Thus, CpG-C treatment and/or loss of mtDNA stimulate the cell to increase the levels of TFAM, which have a strong impact on mitochondria biogenesis (36).

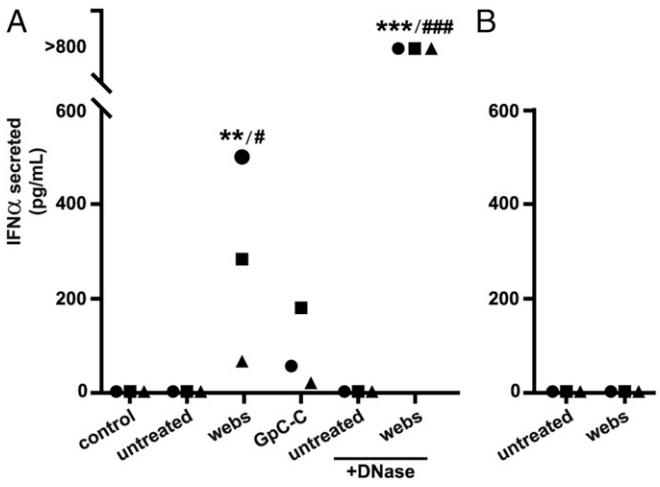

Fig. 4. Webs prime type I IFN secretion. (*A*) IFN-α levels in PBMC cultures were analyzed after 16-h stimulation with web-containing supernatants ("webs") or supernatants from mock-treated CLL cells ("untreated"). PBMCs cultured in fresh medium were used as negative control ("control"). The additional control, GpC-C ODN without cells, was treated in the same way as the web sample ("GpC-C"). Samples were also digested with DNase. (*B*) IFN-α levels in supernatants before PBMC exposure. Data shown represent mean values from three different B-cell web donor preparations (●, ■, and ▲, respectively). The measured IFN-α concentrations for DNase-treated webs were above the linear range for the assay and are viewed as >800 pg/mL. $^{**}P < 0.005$, $^{***}P < 0.0005$, one-way ANOVA followed by Dunnett's post hoc test. $^{\#}P < 0.05$, $^{\#\#\#}P < 0.0005$, one-way ANOVA followed by Sidak's post hoc test for pairwise comparisons (webs vs. GpC-C and webs plus DNase vs. webs).

Discussion

The physiological importance of cell-free circulating mtDNA as a pathogenic factor and DAMP molecule in inflammatory diseases, autoimmunity, cancer, trauma, and bacterial and viral infections, is extensively reviewed in recent publications (3, 7, 24, 37–40). In this study, we report on a previously unrecognized feature of human immune cells: B cells, T cells, NK cells, monocytes, and neutrophils release interferogenic mtDNA webs extracellularly upon exposure to short CpG and non-CpG ODNs of class C. Previously described NET stimuli, such as bacterial lipopolysaccharide (LPS) or PMA, did not generate mtDNA webs. Webs were rapidly released from viable cells, independently of ROS, and were devoid of proteins that trap and kill bacteria, such as granule proteins observed in NETs. Considering the inducing stimuli and effector cell function, our results suggest that lymphocytes utilize mtDNA webs as rapid extracellular messenger molecules and provide alternative roles for mtDNA in antimicrobial signaling.

Derived from a bacterial ancestor, mitochondria share many features with bacteria, including a circular DNA genome with unmethylated CpG motifs (41). As the innate immune system recognizes conserved bacterial molecules, mitochondrial constituents are similarly immunogenic (38, 40, 42). It was previously reported that proinflammatory and antiinflammatory cytokines are produced by activated plasmacytoid dendritic cells and B cells in response to unmethylated CpG-containing DAMP motifs (10, 11). West and Shadel (40) discuss that unique aspects of mtDNA, such as its length, conformation, sequence, and degree of oxidation, govern its differential agonist activities, which may explain why mtDNA release does not uniformly activate both proinflammatory and type I IFN responses (40).

In accordance, we found that the lymphocyte-derived mtDNA webs effectively primed type I IFN production in PBMCs and that enzymatic cleavages of webs into shorter lengths amplified type I IFN response. This finding underlines the interferogenic characteristics of mtDNA previously reported by others (5, 6, 24). Notably, mtDNA is recognized by more than one immune signaling pathway. While Zhang et al. (7) found that mtDNA, released into circulation after injury, activated neutrophils and caused inflammatory responses via TLR9, White et al. (5), Rongvaux et al. (6), and West et al. (4) showed that mtDNA escaping mitochondria during apoptosis or herpes simplex virus 1 exposure, engaged the cGAS/STING signaling pathway to induce type I IFN. Moreover, oxidized mtDNA binds to, and activates, the NLRP3 inflammasome, leading to production of IL-1β (13). mtDNA also promotes neutrophil adhesion and, noteworthy, acts as a potent inducer of NETs that further raise the inflammatory pressure (3, 20, 43). West et al. (4) highlight the role of mtDNA as a participant in cell-intrinsic triggering of innate immune responses and antiviral signaling. Thus, based on these observations, studies by Zhang et al. (7), and our findings, we propose that mtDNA also acts as an extrinsic trigger of innate immune responses.

mtDNA is highly susceptible to oxidation, and oxidized mtDNA is enriched in NETs from systemic lupus erythematosus (SLE) or IFN-primed healthy neutrophils. These oxidized mtDNA induce mRNA expression and secretion of type I IFN, TNF, and IL-6 (24, 44). In autoimmune conditions, besides SLE, increased oxidized mtDNA was found in synovial fluids and plasma of rheumatoid arthritis (45), and in patients with granulomatosis with polyangiitis (46). The pivotal study by Zhang

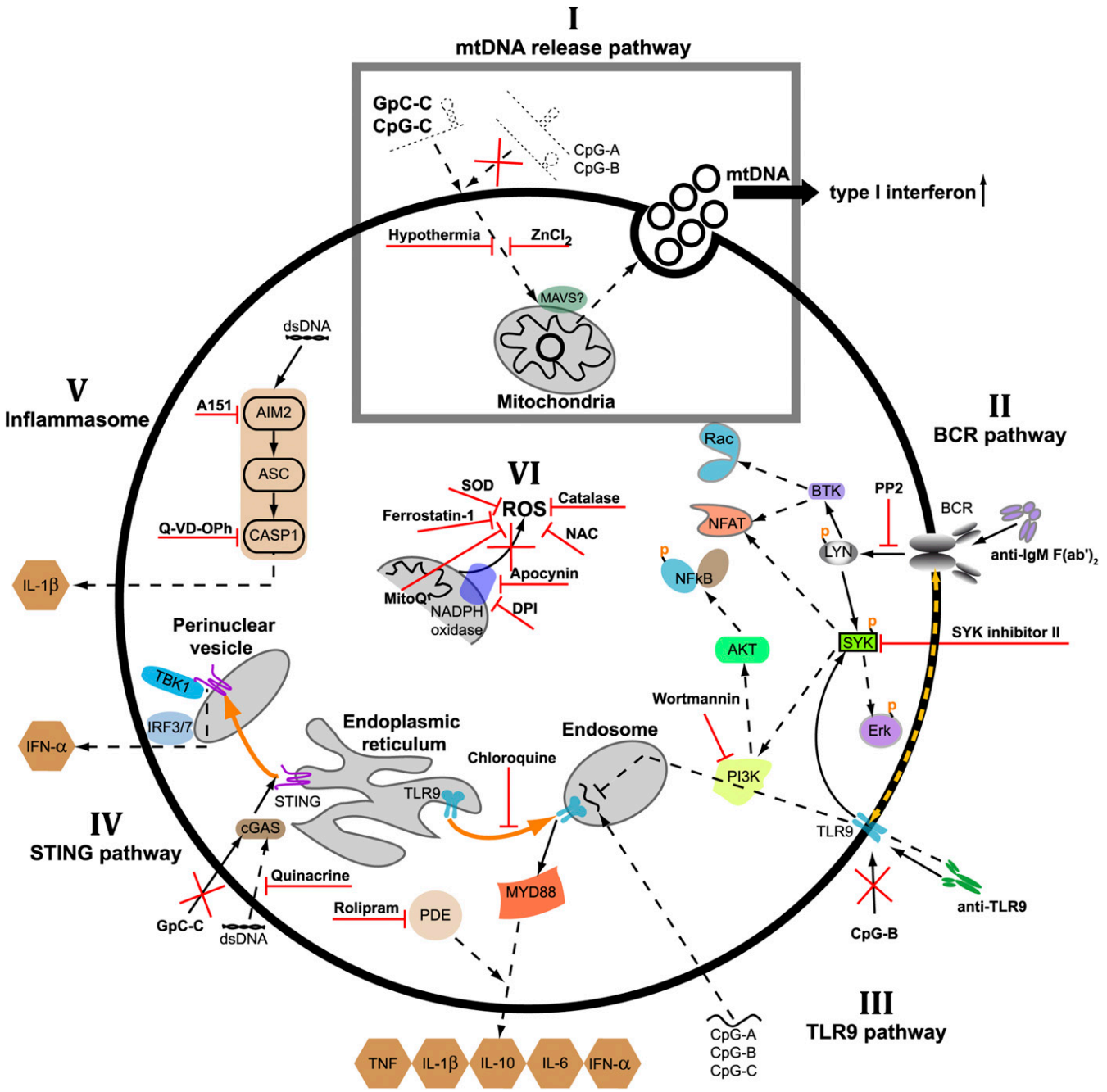

Fig. 5. Summary of pathway analysis. I. Unique signaling pathway responding to CpG-C/GpC-C ODNs. B cells responded to unmethylated CpG-C and GpC-C oligodeoxynucleotides, but not to CpG-A and CpG-B, by releasing mtDNA webs. The release/signal transduction was inhibited by hypothermia and $ZnCl_2$ (Fig. 3*F*). Cyclosporin A act as an inhibitor of mitochondria pore opening and prevents the release of mtDNA fragments. However, the release of mtDNA webs was not inhibited by cyclosporin A (Fig. S4*A*). Endocytosis of CpG-C or GpC-C is apparently not required for B-cell mtDNA web development as two different inhibitors of endocytosis, cytochalasin D and dansylcadaverine, were unable to prevent mtDNA ejection (Fig. S4*A*). II. Evidence for B-cell receptor (BCR) independent pathway. BCR signaling is activated by ligation with anti-IgM $F(ab')_2$. However, treatment of B cells with anti-IgM $F(ab')_2$ did not induce mtDNA release (Fig. 1*G*). Inhibition of BCR downstream signaling molecules, using the inhibitors PP2, Syk inihibitor II, and wortmannin did not hamper mtDNA web release. The targets of these inhibitors, kinases Lyn, Syk, and PI3K, are crucial for BCR signaling acting as transmitters of the activation signal into cytoplasmic signaling pathways (Fig. S4*A*). III. Evidence for TLR9-independent pathway. The most convincing evidence for a TLR9-independent mechanism of mtDNA web release is (*i*) lack of CpG-motif requirement (i.e., also non-CpG-C can stimulate web release) and (*ii*) insensitivity to endosomal inhibitor chloroquine and the fact that cells with low levels of TLR9 can also produce mtDNA webs (Fig. 3 *C* and *E*). See Fig. 3 and connected text for more comprehensive explanation of TLR9 redundancy in web release. IV. Evidence for STING-independent pathway. Stimulation of STING (followed by translocation to perinuclear vesicles) induces type I IFN release. We found no (or weak) type I IFN release from B cells treated with GpC-C, although GpC-C generated mtDNA web release (Fig. S6*B*). Moreover, STING agonist 2′3′-cGAMP did not induce mtDNA web release. Also, quinacrine, a nonspecific inhibitor of STING signaling, did not prevent CpG-C–induced mtDNA web release. We also showed that CLL B cells, despite expressing low levels of STING, could release mtDNA webs (Fig. S6*B*). V. Evidence for AIM2-inflammasome–independent pathway. Inhibition of key enzymes, AIM2 and caspase-1, in inflammasome signaling did not affect mtDNA web release. In addition, IL-1β secretion, normally high upon AIM2 stimulation, was absent or very low in three different donor B-cell samples (Fig. S3*D*). VI. Evidence for ROS-independent mechanism. ROS has a fundamental role in NET release. Inhibitors of ROS formation (i.e., DPI and apocynin) and ROS scavengers (i.e., SOD, catalase, NAC, MitoQ, and ferrostatin-1) did, however, not affect mtDNA web release (Fig. S4*A*). Neither did treatment with inhibitors of mitochondrial electron transport chain and Fenton chemistry (i.e., rotenone and deferoxamine mesylate). See Fig. 6 and related text for more extensive analysis of ROS.

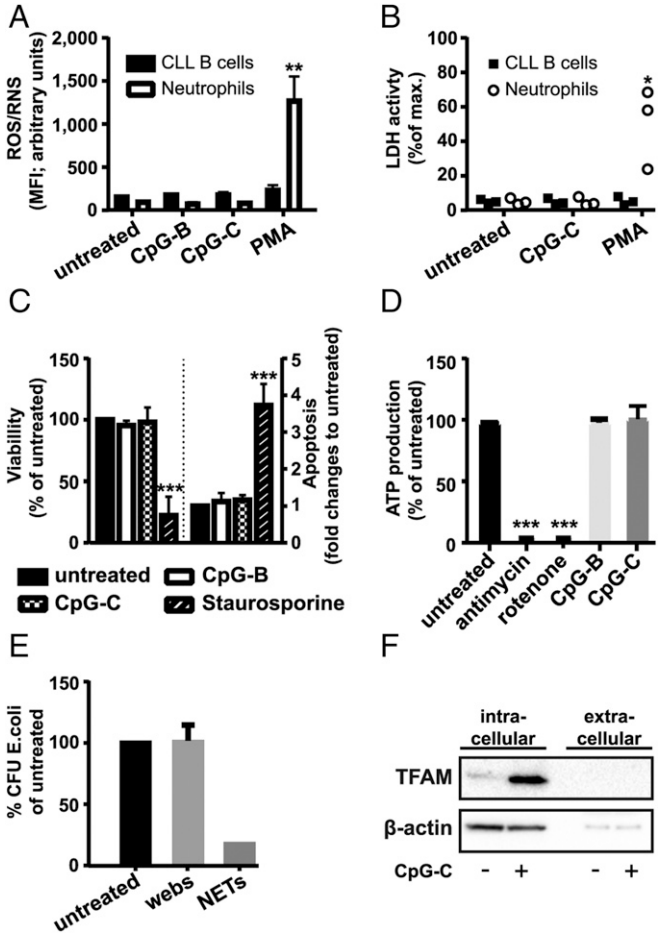

Fig. 6. mtDNA release is ROS and cell death independent. (*A*) Analysis of ROS/RNS formation in CLL B cells and neutrophils exposed to indicated stimuli for 1 h. (*B*) Activity of lactate dehydrogenase (LDH) in cell supernatants after treatment of CLL B cells and neutrophils with CpG-C or PMA was measured as an indicator of necrosis (loss of plasma membrane integrity). LDH activity is expressed as percentage of maximal activity obtained by complete cell lysis. Individual results from three experiments are shown. (*C*) Cell viability and apoptosis were analyzed in the same sample using the ApoTox-Glo Triplex assay. Untreated cells were used as control sample to which all samples were compared ($n = 3$). (*D*) Measurements of ATP production after treatment with CpG-C or CpG-B for 2 h ($n = 3$). ATP production in untreated cells (control) was assumed to be 100%. Inhibitors of mitochondrial electron transport chain, antimycin and rotenone, were used as negative controls. (*E*) The impact of CLL B-cell mtDNA webs on *E. coli* viability (colony formation) was analyzed ($n = 3$). Isolated NETs were included as a control of the assay. The number of colony-forming bacteria in supernatants of untreated CLL B cells was assumed to be 100%. No statistically difference was observed for webs vs. untreated (unpaired *t* test). (*F*) Immunoblot showing the amounts of intracellular and extracellular TFAM levels upon treatment with CpG-C for 4 h. Proteins corresponding to equal number of cells (2×10^5) were separated using SDS/PAGE, and immunoblotting toward actin was used as a loading control. For the extracellular samples, cell culture supernatants from 2×10^5 cells were precipitated and resuspended in SDS/PAGE sample buffer before electrophoresis. Experiments were repeated three times and generated the following CpG-C/untreated ratios for TFAM: 7.6, 6.2, and 26.6. (*A–D*) $*P < 0.05$, $**P < 0.005$, $***P < 0.0005$, one-way ANOVA followed by Dunnett's post hoc test.

et al. (7) showed that circulating mitochondrial-derived formyl peptides and DNA are causing inflammation in response to injury, advocating that the release is a key link between trauma, inflammation, and systemic inflammatory response syndrome. Elevated levels of circulating mtDNA in plasma have also been found in patients during HIV infection. Levels of mtDNA did not correlate with number of T cells nor with markers of immune activation. Significant correlation was, however, observed with plasma virus load, potentially contributing to the chronic inflammatory state observed in the disease (22). Bacterial infections, for example, by *Streptococcus pneumoniae*, increase mtDNA in circulation via TLR9 in acute kidney injury patients (47). Increased mtDNA plasma levels are also observed in cardiovascular conditions, in diseases of aging, and in malignancies (38, 40). Interestingly, our initial observations on mtDNA release were seen in B lymphocytes derived from CLL patients. These were recently shown to have significantly increased mtDNA copy number (48). As noted above, circulating DNA constitute a potential risk for autoantibody induction if not rapidly cleared. Presence of anti-DNA autoantibodies in CLL and SLE (25) underlines the importance of further studies in understanding the impact of mtDNA in the pathogenesis.

Previously, it was reported that fragments of mtDNA escaped from mitochondria into the cytosol by opening of the mitochondrial permeability transition pore, a release that could be blocked by cyclosporin A (28). In contrast, we found that CpG-C stimulated release of full-size mtDNA (e.g., not as fragments) and that discharge was insensitive to cyclosporin A. Although mtDNA was ejected, cell viability, mtDNA copy number, and mitochondrial ATP levels seemed uncompromised in the B cells. The mitochondria holds more copies of mtDNA than required to sustain oxidative phosphorylation, implicating additional roles for mtDNA, possibly related to mitochondrial signaling and immune functions, as suggested (40). High TFAM levels have been shown to correlate with increased mtDNA copy number (35, 49–51). Since we observed unaltered mtDNA copy number along with intense increase of TFAM levels upon CpG-C treatment, it is possible that mitochondria are compensating for the release by mtDNA replication.

Generally, our results suggest that release is an active process and not a result of cell damage. These findings are also supported by the fact that apoptotic pathways, as a rule, do not generate IFN production, whereas we found that CpG-C and GpC-C generated type I IFN production via the release of mtDNA webs, reminiscent of viral infection. In accordance, White and Kile (52) also noted that virally induced mtDNA stress, causing release of mtDNA into the cytosol, is distinct from apoptotic mtDNA release. This may suggest that the GC-rich stem-loop ODNs used in our study are recognized in a pathway that induces mtDNA stress in analogy to certain viruses. Despite recent observations, the mechanism of mtDNA release is still to be clarified, as pointed out recently by West and Shadel (40) and others (4, 52). It is not known how the two levels of mtDNA discharge, first into cytosol then into extracellular space, are regulated (3), but cellular stress is discussed as a primary factor for liberation of mitochondrial DAMPs. Viral infection priming mitochondrial antiviral signaling protein (MAVS)-signalosome located on the outer mitochondrial membrane is probably one of these potent stressors as discussed in detail by Jin et al. (39). Another mechanism was proposed by Caielli et al. (44) who suggested that release of mtDNA requires fusion of mitochondrial membranes with plasma membrane. This hypothesis has, however, yet to be proven.

We speculate that only mitochondria that replicate or transcribe their DNA at the time of CpG-C exposure can eject their DNA. Unlike nuclear DNA, mtDNA is not associated with histones, but organized into compact DNA–protein complexes, nucleoids, which are composed of proteins for mtDNA packaging as well as transcription and replication factors. TFAM plays a key role in the packing of mtDNA into nucleoids. Low levels of TFAM generate a loosely packed nucleoid, while high levels result in a compact state. Transcription of mtDNA occurs when the nucleoid is loose and elongated, while it is inhibited in the compact state (35). Since both our mass spectrometry and immunoblotting analyses showed no concomitant TFAM release along with webs, this implicates

that the level of TFAM physically associated with the mtDNA to be released is low—reminiscent of the loose and elongated nucleoid observed during transcription.

What are the features of the ODNs used in this study? Our finding that webs were released independently of TLR9 was surprising. It is puzzling why three C-class CpG ODNs, both CpG and non-CpG, as well as P-class ODN 21798 generate intense mtDNA web release but not A- and B-classes nor C-class ODN M362. While CpG-motifs are required for cytokine release via TLR9 (53), the CpG motifs are apparently redundant for mtDNA web release. One similarity between web-stimulating ODNs is the predicted GC-rich stem-loop structure present at the 3′, not found in CpG-A, CpG-B, A151, nor ODN M362 (Fig. 4*A* and Fig. S3*F*). It is possible that this 3′ duplex formation is needed for recognition. Recently, Herzner et al. (30) revealed that unique G-rich stem-loop structures, named Y-form DNA, present in endogenous retroviruses and HIV-1, trigger innate cGAS-dependent responses and type I IFN production. The GC-rich structures used in our study contain unpaired guanosines in the closed loop. The structures are not identical but are reminiscent of the short G-rich viral ODNs in Herzner et al.'s study, in which unpaired guanosines are flanking the dsDNA stems. However, we find that the ODNs in our study are devoid of cGAS/STING-stimulatory activity; GpC-C did not induce IFN production and the cGAS/STING inhibitor quinacrine could not inhibit web release. Interestingly, however, albeit the initial signaling routes are distinct, the final outcome in terms of antiviral IFN production, as triggered by webs in our study, is comparable.

Zinc and hypothermia treatments were the only conditions found to prevent liberation of mtDNA webs. As both treatments affect several cellular processes, clues regarding the release mechanism are limited. Zinc is predicted to bind ∼3,000 human proteins (54), and zinc treatment severely impeded mitochondrial functions (i.e., altered metabolism and less ATP production) by inhibiting several mitochondrial enzymes (55). Zinc has also been shown to impair the nucleotide binding ability of a viral-RNA binding protein associated with regulation of MAVS antiviral signaling (56, 57), implicating that zinc similarly may affect recognition of CpG-C and GpC-C by certain DNA sensors. The web-triggering ODN structures used in the present study render further detailed examination including identification of nucleic acid origin (be it modified self-DNA, viral or bacterial DNA) of the stimulating GC-rich ligand and its receptor. Our results contribute to an understanding that the immune system may utilize many different cell populations, a variety of inducing stimuli, and release of mtDNA with discrete compositions/structures to signal danger. mtDNA functions and interactions are still to be explored concerning mode of release and role in antiviral regulation, which are important aspects for understanding mitochondrial interactions with the immune system.

Conclusions

Taken together, our findings that B cells, T cells, and NK cells, as well as monocytes and neutrophils, release mtDNA webs extracellularly in response to certain short GC-rich ODNs, highlight the role of mtDNA as a rapid extrinsic antiviral messenger molecule. These findings accentuate the importance of lymphocyte-derived mtDNA DAMPs in innate immune signaling and should be taken into account when examining the excessive type I IFN production seen in different autoinflammatory diseases and cancer.

Materials and Methods

Ethics Statements. Experiments involving human subjects were done according to the recommendations of the local research ethics committee of Linköping University. Informed consent was obtained from all patients according to the Declaration of Helsinki.

Immune Cell Isolation. PBMCs were isolated from peripheral whole blood drawn from healthy adults and treatment-naive CLL patients by centrifugation in a Ficoll-Hypaque density gradients. B cells, T cells, NK cells, and monocytes were further isolated either by negative or positive selection using microbeads or by flow cytometry. Neutrophils were isolated from peripheral whole blood of healthy adults by gradient centrifugation in Percoll. For detailed description, see *SI Text*.

Stimulation and Visualization of mtDNA Web Formation. A total of 3×10^5 cells per well at a cell density of 2×10^6 cells per mL was seeded in 48-well plates in fresh complete RPMI medium 1640 supplemented with 2% heat-inactivated FBS. Cells were stimulated for 4 h with various immune-stimulating agents (*SI Text*). CpG-C ODN 2395 and ODN 2395 control (GpC-C) (Miltenyi Biotec) were added to cells at a final concentration of 1.25 μg/mL and incubated at 37 °C in 5% CO_2. Released DNA was stained with SYTOX Green (Thermo Fisher Scientific) and visualized using Nikon Eclipse E600W fluorescence microscope equipped with a Nikon DS Ri1 digital camera or with Zeiss Axiovert 200M inverted fluorescence microscope using the AxioCam MRm CCD camera. Degradation of released DNA was generated by addition of DNase I (Sigma-Aldrich) to a final concentration of 10 U/mL and incubation at 37 °C for 30 min.

Collection and Quantification of Extracellular DNA from Cell Supernatants. Following staining of DNA with SYTOX Green and a gentle resuspension, cell supernatants were transferred to microcentrifuge tubes using Sigmacote-treated tips and centrifuged at 1,000 × *g* for 5 min to pellet cells. DNA-containing supernatants were transferred to fresh tubes and dried under vacuum. Dried samples were reconstituted and loaded on 0.8% agarose gels, and DNA was separated with 100 V for 2 h and subsequently imaged in ChemiDoc MP System (Bio-Rad). Relative quantification of the characteristic fragment was done by analyzing band intensities using the Image Lab software (version 4.1; Bio-Rad).

Generation of Webs and Stimulation of PBMCs. A total of 8×10^6 CLL B cells in 4 mL of RPMI 1640 supplemented with 2% FBS was treated or mock treated with 2.5 μg/mL GpC-C for 4 h before supernatants were collected and centrifuged (300 × *g* for 5 min followed by 4,000 × *g* for 5 min). Subsequently, supernatants were washed twice with PBS in Amicon Ultra-30 filter devices (Merck Millipore). Samples were split in two, of which one was treated with DNase before three additional PBS washes in Amicon Ultra-30. After the final wash, samples were volume-adjusted with RPMI 1640. GpC-C in RPMI 1640 supplemented with 2% FBS without cells was treated in the same way as the non-DNase–treated samples. Aliquots were saved for analysis of IFN-α.

A total of 1×10^6 isolated healthy donor PBMCs was incubated with the above-described samples for 16 h at 37 °C in 200 μL of RPMI 1640 supplemented with 5% FBS. A negative control, PBMCs in fresh cell culture media were also included. Samples were run in duplicates on three occasions using different CLL B-cell and PBMC donors. Following incubation, cell supernatants were collected by centrifugation at 300 × *g* for 5 min before IFN-α2 levels were analyzed using ELISAs (Mabtech) according to the manufacturer's recommendation.

Statistical Methods. Statistical calculations were performed using GraphPad Prism, version 7.03 (GraphPad Software). For the statistical analysis of three or more groups, one-way ANOVA was applied followed by Dunnett's post hoc test for multiple comparison or Sidak's post hoc test for pairwise comparisons. Differences between two groups were assessed using Student's *t* test. Statistically significant differences were indicated with asterisks: $^{*}P < 0.05$, $^{**}P < 0.005$, or $^{***}P < 0.0005$. In Figs. 3*B* and 4, significant differences for pairwise comparisons are indicated with a number sign: $^{\#}P < 0.05$ or $^{\#\#\#}P < 0.0005$.

Additional methods used in the manuscript can be found as *SI Text*.

ACKNOWLEDGMENTS. We are grateful to Dr. Maria V. Turkina in the mass spectrometry core facility (Faculty of Medicine, Linköping University) for professional support. We thank Drs. Marie Larsson, Jonas Blomberg, Colm Nestor, Mikael Lindgren, and Ida Eriksson for valuable comments on the manuscript. This work was financed by grants from the Linköping Medical Society (to B.I. and A.-C.B.); Linköping University and ALF grants, Region Östergötland, Sweden (to A.R.); Linköping University Cancer start-up grant (to A.R.); and Ingrid Asp Foundation (M.S.) and Swedish Cancer Society.

1. Paludan SR, Bowie AG (2013) Immune sensing of DNA. *Immunity* 38:870–880.
2. Takeuchi O, Akira S (2010) Pattern recognition receptors and inflammation. *Cell* 140: 805–820.
3. Nakahira K, Hisata S, Choi AM (2015) The roles of mitochondrial damage-associated molecular patterns in diseases. *Antioxid Redox Signal* 23:1329–1350.
4. West AP, et al. (2015) Mitochondrial DNA stress primes the antiviral innate immune response. *Nature* 520:553–557.
5. White MJ, et al. (2014) Apoptotic caspases suppress mtDNA-induced STING-mediated type I IFN production. *Cell* 159:1549–1562.
6. Rongvaux A, et al. (2014) Apoptotic caspases prevent the induction of type I interferons by mitochondrial DNA. *Cell* 159:1563–1577.
7. Zhang Q, et al. (2010) Circulating mitochondrial DAMPs cause inflammatory responses to injury. *Nature* 464:104–107.
8. Krieg AM, et al. (1995) CpG motifs in bacterial DNA trigger direct B-cell activation. *Nature* 374:546–549.
9. Klinman DM, Yi AK, Beaucage SL, Conover J, Krieg AM (1996) CpG motifs present in bacteria DNA rapidly induce lymphocytes to secrete interleukin 6, interleukin 12, and interferon gamma. *Proc Natl Acad Sci USA* 93:2879–2883.
10. Bauer S, et al. (2001) Human TLR9 confers responsiveness to bacterial DNA via species-specific CpG motif recognition. *Proc Natl Acad Sci USA* 98:9237–9242.
11. Hemmi H, et al. (2000) A Toll-like receptor recognizes bacterial DNA. *Nature* 408: 740–745.
12. Nakahira K, et al. (2011) Autophagy proteins regulate innate immune responses by inhibiting the release of mitochondrial DNA mediated by the NALP3 inflammasome. *Nat Immunol* 12:222–230.
13. Shimada K, et al. (2012) Oxidized mitochondrial DNA activates the NLRP3 inflammasome during apoptosis. *Immunity* 36:401–414.
14. Brinkmann V, et al. (2004) Neutrophil extracellular traps kill bacteria. *Science* 303: 1532–1535.
15. Fuchs TA, et al. (2007) Novel cell death program leads to neutrophil extracellular traps. *J Cell Biol* 176:231–241.
16. Morshed M, et al. (2014) NADPH oxidase-independent formation of extracellular DNA traps by basophils. *J Immunol* 192:5314–5323.
17. Yousefi S, et al. (2008) Catapult-like release of mitochondrial DNA by eosinophils contributes to antibacterial defense. *Nat Med* 14:949–953.
18. Yousefi S, Mihalache C, Kozlowski E, Schmid I, Simon HU (2009) Viable neutrophils release mitochondrial DNA to form neutrophil extracellular traps. *Cell Death Differ* 16:1438–1444.
19. Yousefi S, et al. (2015) Basophils exhibit antibacterial activity through extracellular trap formation. *Allergy* 70:1184–1188.
20. Itagaki K, et al. (2015) Mitochondrial DNA released by trauma induces neutrophil extracellular traps. *PLoS One* 10:e0120549.
21. Thieblemont N, Wright HL, Edwards SW, Witko-Sarsat V (2016) Human neutrophils in auto-immunity. *Semin Immunol* 28:159–173.
22. Cossarizza A, et al. (2011) Increased plasma levels of extracellular mitochondrial DNA during HIV infection: A new role for mitochondrial damage-associated molecular patterns during inflammation. *Mitochondrion* 11:750–755.
23. Liu S, Feng M, Guan W (2016) Mitochondrial DNA sensing by STING signaling participates in inflammation, cancer and beyond. *Int J Cancer* 139:736–741.
24. Lood C, et al. (2016) Neutrophil extracellular traps enriched in oxidized mitochondrial DNA are interferogenic and contribute to lupus-like disease. *Nat Med* 22:146–153.
25. Sthoeger ZM, et al. (1989) Production of autoantibodies by CD5-expressing B lymphocytes from patients with chronic lymphocytic leukemia. *J Exp Med* 169:255–268.
26. Lanemo Myhrinder A, et al. (2008) A new perspective: Molecular motifs on oxidized LDL, apoptotic cells, and bacteria are targets for chronic lymphocytic leukemia antibodies. *Blood* 111:3838–3848.
27. Bergh AC, et al. (2014) Silenced B-cell receptor response to autoantigen in a poor-prognostic subset of chronic lymphocytic leukemia. *Haematologica* 99:1722–1730.
28. Patrushev M, et al. (2004) Mitochondrial permeability transition triggers the release of mtDNA fragments. *Cell Mol Life Sci* 61:3100–3103.
29. Verthelyi D, Zeuner RA (2003) Differential signaling by CpG DNA in DCs and B cells: Not just TLR9. *Trends Immunol* 24:519–522.
30. Herzner AM, et al. (2015) Sequence-specific activation of the DNA sensor cGAS by Y-form DNA structures as found in primary HIV-1 cDNA. *Nat Immunol* 16:1025–1033.
31. Tan Y, et al. (2015) Inhibition of type 4 cyclic nucleotide phosphodiesterase blocks intracellular TLR signaling in chronic lymphocytic leukemia and normal hematopoietic cells. *J Immunol* 194:101–112.
32. Ishii KJ, et al. (2002) Potential role of phosphatidylinositol 3 kinase, rather than DNA-dependent protein kinase, in CpG DNA-induced immune activation. *J Exp Med* 196: 269–274.
33. Guerrier T, et al. (2014) TLR9 expressed on plasma membrane acts as a negative regulator of human B cell response. *J Autoimmun* 51:23–29.
34. Urban CF, et al. (2009) Neutrophil extracellular traps contain calprotectin, a cytosolic protein complex involved in host defense against *Candida albicans*. *PLoS Pathog* 5: e1000639.
35. Kukat C, et al. (2015) Cross-strand binding of TFAM to a single mtDNA molecule forms the mitochondrial nucleoid. *Proc Natl Acad Sci USA* 112:11288–11293.
36. Picca A, Lezza AM (2015) Regulation of mitochondrial biogenesis through TFAM-mitochondrial DNA interactions: Useful insights from aging and calorie restriction studies. *Mitochondrion* 25:67–75.
37. Weinberg SE, Sena LA, Chandel NS (2015) Mitochondria in the regulation of innate and adaptive immunity. *Immunity* 42:406–417.
38. Boyapati RK, Tamborska A, Dorward DA, Ho GT (2017) Advances in the understanding of mitochondrial DNA as a pathogenic factor in inflammatory diseases. *F1000Res* 6:169.
39. Jin HS, Suh HW, Kim SJ, Jo EK (2017) Mitochondrial control of innate immunity and inflammation. *Immune Netw* 17:77–88.
40. West AP, Shadel GS (2017) Mitochondrial DNA in innate immune responses and inflammatory pathology. *Nat Rev Immunol* 17:363–375.
41. Hong EE, Okitsu CY, Smith AD, Hsieh CL (2013) Regionally specific and genome-wide analyses conclusively demonstrate the absence of CpG methylation in human mitochondrial DNA. *Mol Cell Biol* 33:2683–2690.
42. Collins LV, Hajizadeh S, Holme E, Jonsson IM, Tarkowski A (2004) Endogenously oxidized mitochondrial DNA induces in vivo and in vitro inflammatory responses. *J Leukoc Biol* 75:995–1000.
43. Sørensen OE, Borregaard N (2016) Neutrophil extracellular traps—the dark side of neutrophils. *J Clin Invest* 126:1612–1620.
44. Caielli S, et al. (2016) Oxidized mitochondrial nucleoids released by neutrophils drive type I interferon production in human lupus. *J Exp Med* 213:697–713.
45. Hajizadeh S, DeGroot J, TeKoppele JM, Tarkowski A, Collins LV (2003) Extracellular mitochondrial DNA and oxidatively damaged DNA in synovial fluid of patients with rheumatoid arthritis. *Arthritis Res Ther* 5:R234–R240.
46. Surmiak MP, et al. (2015) Circulating mitochondrial DNA in serum of patients with granulomatosis with polyangiitis. *Clin Exp Immunol* 181:150–155.
47. Tsuji N, et al. (2016) Role of mitochondrial DNA in septic AKI via Toll-like receptor 9. *J Am Soc Nephrol* 27:2009–2020.
48. Hosnijeh FS, et al. (2014) Mitochondrial DNA copy number and future risk of B-cell lymphoma in a nested case-control study in the prospective EPIC cohort. *Blood* 124: 530–535.
49. Ekstrand MI, et al. (2004) Mitochondrial transcription factor A regulates mtDNA copy number in mammals. *Hum Mol Genet* 13:935–944.
50. Ikeda M, et al. (2015) Overexpression of TFAM or twinkle increases mtDNA copy number and facilitates cardioprotection associated with limited mitochondrial oxidative stress. *PLoS One* 10:e0119687.
51. Chakrabarty S, et al. (2014) Upregulation of TFAM and mitochondria copy number in human lymphoblastoid cells. *Mitochondrion* 15:52–58.
52. White MJ, Kile BT (2015) Stressed mitochondria sound the alarm. *Immunol Cell Biol* 93:427–428.
53. Vollmer J, et al. (2004) Characterization of three CpG oligodeoxynucleotide classes with distinct immunostimulatory activities. *Eur J Immunol* 34:251–262.
54. Maret W (2013) Zinc biochemistry: From a single zinc enzyme to a key element of life. *Adv Nutr* 4:82–91.
55. Lemire J, Mailloux R, Appanna VD (2008) Zinc toxicity alters mitochondrial metabolism and leads to decreased ATP production in hepatocytes. *J Appl Toxicol* 28: 175–182.
56. Yabe-Wada T, et al. (2016) TLR signals posttranscriptionally regulate the cytokine trafficking mediator sortilin. *Sci Rep* 6:26566.
57. Zhou X, You F, Chen H, Jiang Z (2012) Poly(C)-binding protein 1 (PCBP1) mediates housekeeping degradation of mitochondrial antiviral signaling (MAVS). *Cell Res* 22: 717–727.
58. Söderberg D, et al. (2015) Increased levels of neutrophil extracellular trap remnants in the circulation of patients with small vessel vasculitis, but an inverse correlation to anti-neutrophil cytoplasmic antibodies during remission. *Rheumatology (Oxford)* 54: 2085–2094.
59. Malik AN, Shahni R, Rodriguez-de-Ledesma A, Laftah A, Cunningham P (2011) Mitochondrial DNA as a non-invasive biomarker: Accurate quantification using real time quantitative PCR without co-amplification of pseudogenes and dilution bias. *Biochem Biophys Res Commun* 412:1–7.
60. Buenrostro JD, Giresi PG, Zaba LC, Chang HY, Greenleaf WJ (2013) Transposition of native chromatin for fast and sensitive epigenomic profiling of open chromatin, DNA-binding proteins and nucleosome position. *Nat Methods* 10:1213–1218.
61. Langmead B, Trapnell C, Pop M, Salzberg SL (2009) Ultrafast and memory-efficient alignment of short DNA sequences to the human genome. *Genome Biol* 10:R25.
62. Langmead B, Salzberg SL (2012) Fast gapped-read alignment with Bowtie 2. *Nat Methods* 9:357–359.
63. Heinz S, et al. (2010) Simple combinations of lineage-determining transcription factors prime *cis*-regulatory elements required for macrophage and B cell identities. *Mol Cell* 38:576–589.
64. Kent WJ, et al. (2002) The human genome browser at UCSC. *Genome Res* 12: 996–1006.
65. Nesvizhskii AI, Keller A, Kolker E, Aebersold R (2003) A statistical model for identifying proteins by tandem mass spectrometry. *Anal Chem* 75:4646–4658.